Electronic structure of oxygen-terminated zigzag graphene nanoribbons: A hybrid density functional theory study

Ashwin Ramasubramaniam*
Department of Mechanical and Industrial Engineering, University of Massachusetts, Amherst, Massachusetts 01003, USA
(Received 13 April 2010; revised manuscript received 14 May 2010; published 9 June 2010)

The size-dependent electronic structure of oxygen-terminated zigzag graphene nanoribbons is investigated using standard density functional theory (DFT) with an exchange-correlation functional of the generalized gradient approximation form as well as hybrid DFT calculations with two different exchange-correlation functionals. Hybrid DFT calculations, which typically provide more accurate band gaps than standard DFT, are found to predict *semiconducting* behavior in oxygen-terminated zigzag graphene nanoribbons; this is in distinct contrast to standard DFT with (semi)local exchange-correlation functionals, which have been widely employed in previous studies and shown to predict *metallic* behavior. (Semi)local exchange-correlation functionals employed in standard DFT calculations cause unphysical delocalization of lone pairs from the oxygen atoms due to self-interaction errors and lead to metallic behavior. Hybrid DFT calculations do not suffer from this spurious effect and produce a clear size-dependent band gap. Appreciable fundamental band gaps (~ 1 eV) are found for the smallest ribbons (two zigzag rows); the band gap decreases rapidly with increasing ribbon width, resulting eventually in a zero band-gap semiconductor at about 4–5 zigzag rows. This finding could have useful implications for molecular electronics, in particular, since oxygen-terminated zigzag graphene nanoribbons are thermodynamically stable unlike their hydrogenated counterparts. More generally, through a concrete example, this study suggests caution when employing (semi)local functionals in DFT studies of functionalized graphene/graphene derivatives when the functional groups contain electron lone pairs.

DOI: 10.1103/PhysRevB.81.245413 PACS number(s): 73.22.Pr

I. INTRODUCTION

Graphene, or single layer graphite, is a promising material for the next generation of electronic devices as well as an excellent testing ground for theories of low-dimensional physics.[1,2] Graphene nanoribbons (GNRs), in particular, have been the subject of extensive experimental[3,4] and theoretical[5–9] research due to their unique electronic properties. Quantum confinement of charge carriers in GNRs, which are essentially quasi-one-dimensional structures, leads to the opening of an energy gap that scales inversely with ribbon width.[3,4,6,10] Chemical modification of the edges of GNRs has also been explored as an means of modifying their electronic properties.[7,8] The ability to tune the properties of GNRs, both via structure and chemistry, makes them versatile candidates for carbon-based electronics.

The electronic properties of GNRs stem from quantum confinement of charge carriers as well as the presence of edges. GNRs with zigzag edges (ZGNRs) develop small band gaps due to a staggered sublattice potential arising from spin-ordered states at the edges.[6] These edge states are localized close to the Fermi level. Armchair GNRs (AGNRs) do not display such edge states and follow the same rules for metallic or semiconducting behavior as single-wall carbon nanotubes.[6,11] Thus, structural and chemical modification along edges is likely to have a greater influence on the properties of ZGNRs over AGNRs.[5] The influence of edge chemistry on the electronic properties of ZGNRs, arising from different terminations[5,7,8,12] and substitution of edge atoms,[7] has been examined extensively in theoretical studies. Among various edge terminations considered in these studies, oxygen termination of ZGNRs is of particular relevance when ZGNRs are produced via chemical routes such as oxygen plasma etching[3,4] or oxidative cutting of carbon nanotubes.[13,14] Previous density functional theory (DFT) calculations with (semi)local functionals[5,12] indicate that edge oxygen atoms eliminate the band gap in ZGNRs and render them metallic. Thus, O-terminated GNRs were deemed undesirable for digital electronics applications where semiconducting behavior is typically preferred.

While the aforementioned DFT studies[5,12] indicate that O-terminated ZGNRs (O-ZGNRs) are metallic, there is a discrepancy between DFT studies that use the local (spin) density approximation (LSDA) or the generalized gradient approximation (GGA), and the hybrid DFT study by Hod *et al.*[8] who reported a small band gap (~ 0.03 eV) for an O-ZGNR with eight zigzag rows. Also, if an O-ZGNR can indeed exhibit a band gap, which we will see later is the case, the issue of how the electronic structure of the O-ZGNR is affected by ribbon width remains unexplored, in part because all of the above studies were conducted on ZGNRs with a fixed width (typically $N=8$ rows). In contrast, H-terminated ZGNRs (H-ZGNRs) have been examined in more detail. In a recent study, Jiang *et al.*[9] have shown that the characteristic antiferromagnetic ground state of H-ZGNRs persists up to a width of $N=2$ zigzag rows (polyacene) as does the inverse correlation of band gap and width. For $N=1$ (trans-polyacetylene), there is no longer a magnetic ground state although there is still a large band gap of about 1.2 eV. The addition of a second zigzag row of carbon atoms provides a hexagonal ring for the C π electrons to localize and form magnetic order. A similar systematic analysis of size-dependent properties of O-ZGNRs is the focus of this paper.

In what follows, I study the size-dependent electronic structure of O-ZGNRs for $N=2-5$ (henceforth abbreviated as O-N-ZGNR) using both standard and hybrid DFT.[15] Stan-

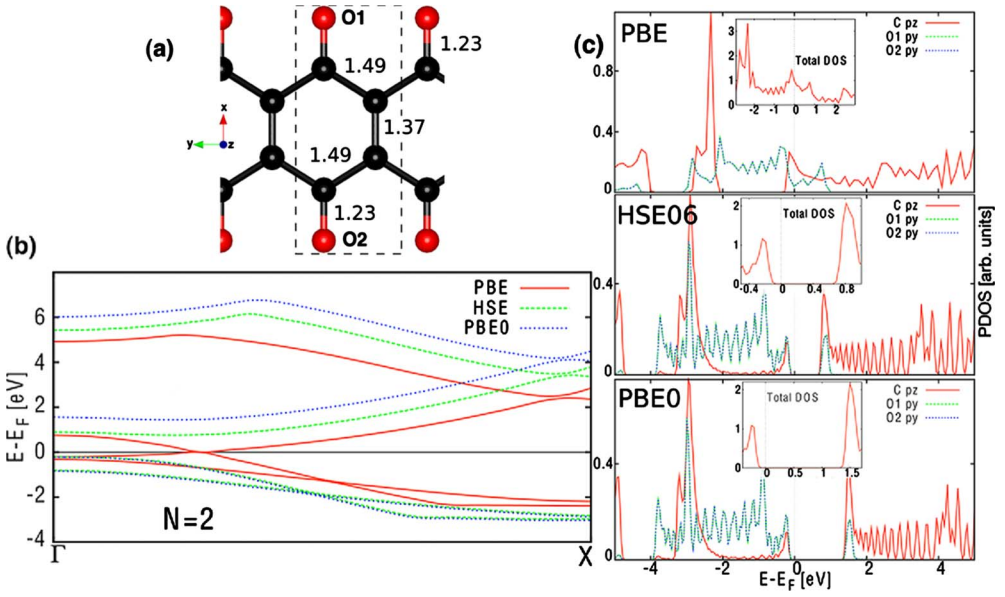

FIG. 1. (Color online) (a) Schematic of O-2-ZGNR; C and O atoms are denoted by black and red spheres, respectively. The dotted lines enclose a repeating periodic unit. Bond lengths (Å) are also indicated. (b) Band structure for O-2-ZGNR computed with PBE (solid red lines), HSE06 (dashed green lines), and PBE0 (dotted blue lines) XC functionals. (c) Partial density of states for the p_y orbitals (lone pair) of the two O atoms [labeled O1 and O2 in (a)] and for the p_z orbitals summed over all C atoms. Since the two spin channels are degenerate, the band structure and density of states are only plotted for the majority spin.

dard DFT with (semi)local exchange-correlation (XC) functionals is known to suffer from self-interaction errors leading to excessive delocalization of electrons;[16] as we will see in the following, this spurious behavior leads to unexpected metallic behavior in O-ZGNRs. Hybrid density functionals reduce the self-interaction error by mixing in a fraction of Hartree-Fock exchange and significantly improve many electronic properties. In particular, hybrid DFT calculations provide band gaps that are more accurate than standard DFT.[17] Hence, both standard and hybrid DFT are compared and contrasted in this work. I show here that there is a discontinuous transition from a nonmagnetic state to an antiferromagnetic ground state as the number of zigzag rows increases from $N=2$ to $N=3$. The electronic band structure and precise band gap of an O-ZGNR is found to depend quite sensitively upon the XC functional employed. Hybrid DFT calculations indicate that O-ZGNRs become *zero band-gap semiconductors* with increasing N in distinct contrast to LSDA/GGA-based DFT calculations, which always predict metallic behavior for O-ZGNRs. The implications of this important finding are discussed in further detail in Sec. III.

II. COMPUTATIONAL METHODOLOGY

DFT calculations are performed using the Vienna *ab initio* simulation package[18] with the projector augmented wave[19,20] method. Within standard DFT, the Perdew-Burke-Ernzerhof (PBE) (Ref. 21) form of the GGA is employed to describe electron exchange and correlation. Hybrid DFT calculations are performed with the PBE0 XC functional[22] and the screened-exchange Heyd-Scuseria-Ernzerhof (HSE06) functional.[23] ZGNRs with $N=2-5$ zigzag rows [e.g., Fig. 1(a)] are modeled within the supercell approach with at least 10 Å of vacuum in the nonperiodic directions. All atoms and cell vectors are relaxed first in a paramagnetic calculation with a force tolerance of 0.02 eV/Å. Thereafter, the band structure and density of states are obtained with a kinetic-energy cutoff of 500 eV, a $1\times45\times1$ Γ-centered k-point mesh, and a Gaussian smearing of the Fermi surface of 0.05 eV.

The magnetic ground state of the O-ZGNR is sensitive to the initial conditions. Depending upon the initial magnetic state (ferromagnetic/antiferromagnetic) it is possible to converge to either a metastable ferromagnetic state or a stable antiferromagnetic ground state for $N\geq3$. The ferromagnetic states are typically higher in energy by a few millielectron volts per unit cell than the antiferromagnetic states, as noted in previous work as well,[8,9] and will not be considered further in this work.

III. RESULTS AND DISCUSSION

We begin by considering an O-2-ZGNR whose structure is displayed in Fig. 1(a). This structure is essentially a polymer of 1,4-benzoquinone in the same way that an H-2-ZGNRs may be considered a polyacene.[9] As seen from the energy of formation on a per atom basis in Table I, the structure is thermodynamically stable with respect to its constituents. In contrast to an unterminated 2-ZGNR or H-2-ZGNR, both of which display antiferromagnetic coupling of the two graphene sublattices, the O-2-ZGNR is nonmagnetic (independent of both level of theory and XC functional). This is entirely expected: since the p_z electrons of the edge C atoms participate in π bonds with the O atoms, there is no longer an arene-like hexagonal ring of C π electrons that can localize on the two graphene sublattices and form magnetic order.

TABLE I. Comparison of the relative stability and band gaps of O-ZGNRs with varying number of zigzag rows (N) for standard and hybrid DFT with various XC functionals. The relative stability of each structure is inferred from the change in energy per atom, ΔE, of the structure with respect to its constituents; graphene and the triplet state of the O_2 molecule are the reference states. Values of electronic band gaps are indicated where applicable. We distinguish between a near-zero gap, in which case the O-ZGNR is a near-zero band-gap semiconductor, and metallic cases when bands actually cross the Fermi level.

	ΔE (eV/atom)			Band gap (eV)		
N	PBE	HSE06	PBE0	PBE	HSE06	PBE0
2	−0.20	−0.12	−0.10	Metallic	0.71	1.40
3	−0.14	−0.05	−0.04	Metallic	0–0.04	0.35
4	−0.11	−0.04	−0.03	Metallic	~0	0.20
5	−0.09	−0.03	−0.02	Metallic	~0	~0

The smallest size of ZGNR for which antiferromagnetic coupling of the graphene sublattices occurs is $N=3$, as discussed later. Of greater interest, is the electronic structure of the O-2-ZGNR, which is shown in detail in Figs. 1(b) and 1(c). From the band structure plot [Fig. 1(b)], we see significant *qualitative* differences between standard and hybrid DFT—as evident, the former predicts metallic behavior for the O-2-ZGNR whereas the latter predicts semiconducting behavior. The top of the valence band and the bottom of the conduction band clearly move away from the Fermi level with both PBE0 and HSE06 calculations and open up an indirect band gap (between the Γ point and $k \approx 0.23\pi/a$) of 0.71 eV and 1.4 eV, respectively (Table I). A clearer understanding of the electronic structure may be obtained by analyzing the partial density of states as shown in Fig. 1(c). For convenience, only contributions from atomic orbitals that lead to a significant density of states near the Fermi level are displayed, namely, the p_y lone pairs on the edge O atoms and the p_z orbitals from the C atoms. As seen in Fig. 1(c), there is a clear qualitative difference between standard and hybrid DFT calculations. The PBE XC functional delocalizes the oxygen p_y lone pairs leading to a finite density of states at the Fermi level. This is clearly unphysical since the p_y lone pairs are in the plane of the ZGNR and ought not to delocalize (e.g., by participating in an aromatic system). One should expect the nonbonding electrons in the O p_y orbitals to be localized, possibly toward the top of the valence band, but definitely below the Fermi level. Furthermore, there is also a finite density of states arising from the C p_z orbitals at the Fermi level, which is again unphysical. Electrons in the p_z orbitals of the edge C atoms participate in a π bond with the O atoms; the inner C atoms also form π bonds between themselves. Therefore, one does not expect delocalized electrons from the C p_z orbitals at the Fermi level. In distinct contract, hybrid DFT calculations with both PBE0 and HSE06 clearly localize the O p_y states just below the Fermi level. Furthermore, there are no C p_z states at the Fermi level and we see clear evidence of a band gap; the gap may be seen more clearly in the insets of Fig. 1(c), which display the total density of states near the Fermi level. Apparently, standard DFT with the PBE XC functional causes excessive delocalization of electrons leading to unphysical results; the inclusion of a fraction of nonlocal exact exchange within the hybrid approach appears to alleviate this problem.

Next, we consider the electronic structure of an O-3-ZGNR (Fig. 2). The O-3-ZGNR is the smallest ZGNR for which antiferromagnetic coupling of the two graphene sublattices is observed [Fig. 2(a)]. As seen from Fig. 2(b), there is once again an obvious difference between standard and hybrid DFT calculations: the former clearly produces a metallic band structure for the O-3-ZGNR whereas the latter predicts semiconducting behavior. Interestingly, both HSE06 and PBE0 XC functionals predict a band gap at $k \approx 0.38\pi/a$, which is approximately where one of the bands crosses the Fermi level in the standard DFT calculation. Again, from the partial density of states plots [Fig. 2(c)], we see that standard DFT with the PBE XC functional delocalizes the O p_y lone pairs and produces a finite density of states at the Fermi level from these lone pairs as well as the C p_z orbitals. In contrast, hybrid DFT calculations with PBE0 and HSE06 XC functionals show zero density of states at the Fermi level. The p_y lone pair from one of the O atoms is clearly well localized below the Fermi level; the lone pair from the other O atom now seems to show a non-negligible density of states in the conduction band. Since there is significant crowding of states near the Fermi level from the O lone pairs as well as the C p_z orbitals (the latter increasing with additional zigzag rows), it is possible that the density of states in the vicinity of the Fermi level is highly sensitive to numerical parameters such as energy cutoff, k-point sampling, smearing, and the size of the Wigner-Seitz cell used for projection of states onto atomic orbitals. Additional studies might serve to shed light on these issues although it must be noted that the parameters used in this study already entail fairly high computational cost for hybrid DFT calculations. These details notwithstanding, it is amply clear in going from $N=2$ to $N=3$ zigzag rows, that hybrid DFT calculations still predict semiconducting behavior albeit with a reduced band gap of 0.35 eV with PBE0 and ≤ 40 meV with HSE06 XC functionals [see insets of Fig. 2(c)].

Finally, we analyze the electronic structure of O-4-ZGNR and O-5-ZGNR in Figs. 3(a) and 3(b), respectively. For the O-4-ZGNR the band gap closes at $k \approx 0.41\pi/a$ with the HSE06 XC functional whereas there is still a small gap of

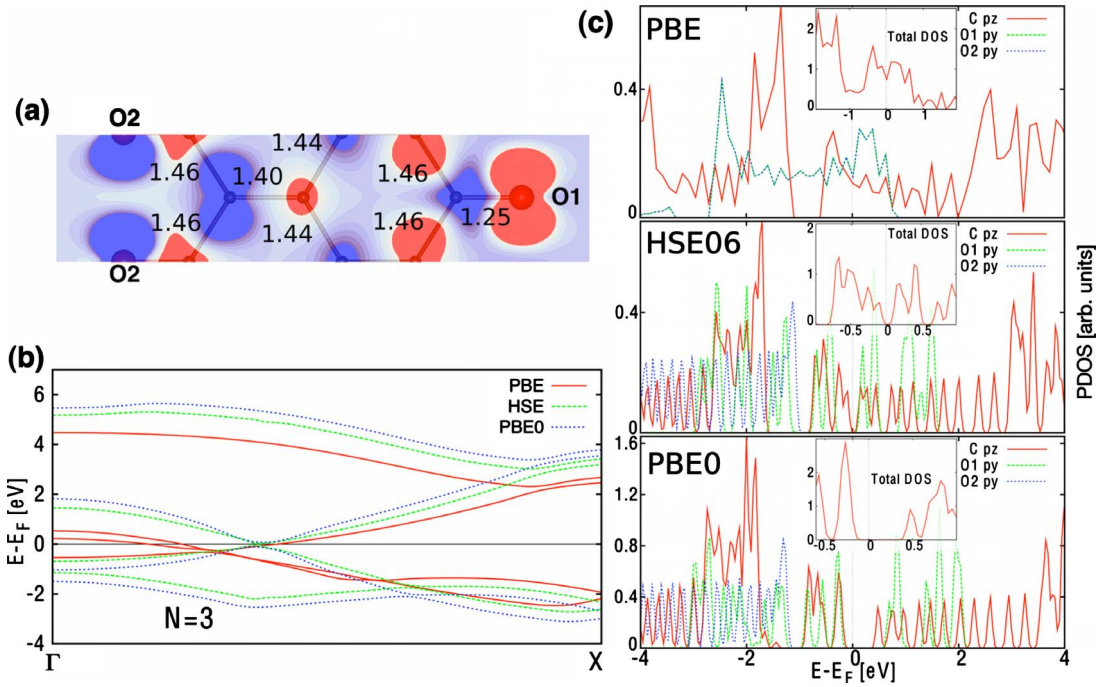

FIG. 2. (Color online) (a) Contours of integrated spin density (with HSE06 XC functional) projected on the plane of the ZGNR; red (blue) regions indicate spin densities greater (lesser) than 0.02(−0.02) $e/\text{Å}^2$. Bond lengths (Å) are also indicated. (b) Band structure for O-3-ZGNR computed with PBE (solid red lines), HSE06 (dashed green lines), and PBE0 (dotted blue lines) XC functionals. (c) Partial density of states for the p_y orbitals (lone pair) of the two O atoms [labeled O1 and O2 in (a)] and for the p_z orbitals summed over all C atoms. Since the two spin channels are degenerate, the band structure and density of states are only plotted for the majority spin.

0.2 eV at the same k point with the PBE0 XC functional. Eventually, for the O-5-ZGNR, the band gap closes with both HSE06 and PBE0 XC functionals. For both the O-4-ZGNR and O-5-ZGNR, we once again see that the standard DFT with the PBE XC functional continues to produce delocalized O p_y and C p_z states at the Fermi level. In contrast, the hybrid DFT calculations produce a zero density of states at the Fermi level. The band structures (which are not shown here for brevity) are qualitatively similar to the $N=3$ case—bands cross the Fermi level in standard DFT calculations whereas the valence and conduction band progressively approach each other tending toward a zero band gap without actually crossing the Fermi level for the hybrid calculations.

From the above results, the following conclusions may be drawn about the electronic properties of O-ZGNRs with respect to both the width of the GNR as well as the level of theory used in the calculations. First, we see that standard DFT with the PBE XC functional consistently predicts metallic behavior for O-ZGNRs. This is not a flaw of GGA alone: previous DFT studies with LSDA also report similar behavior.[5,12] However, hybrid DFT calculations with the HSE06 and PBE0 XC functionals predict decreasing band gaps with increasing ribbon width, ultimately leading to a zero band-gap semiconductor. Indeed, in a previous study of various edge functionalizations of an 8-ZGNR, Hod *et al.*[8] have also reported a very small band gap of 0.03 eV for the 8-O-ZGNR (ketonated ZGNR in their paper) with the HSE06 XC functional.[24] Clearly, (semi)local XC functionals (LSDA/GGA) employed in standard DFT calculations excessively delocalize the O p_y lone pair electrons, as seen above, which in turn interact with the C p_z electrons and lead to a finite density of states at the Fermi level and thence metallic behavior. It is worth noting that similar errors associated with LSDA/GGA have been reported in other contexts (e.g., in the work of Dori *et al.*[25] on the electronic structure of 3,4,9,10-perylene tetracarboxylic dianhydride) and have been discussed at length in the review article by Kronik and Kümmel.[16] In a nutshell, LSDA/GGA are prone to self-interaction errors, which become particularly significant when Kohn-Sham orbitals are localized, as is the case with lone pairs on the O atoms here. The spurious self-interaction destabilizes these localized orbitals, incorrectly delocalizes electrons, and produces both a *qualitatively* and *quantitatively* incorrect picture of the electronic structure of O-ZGNRs. Hybrid DFT calculations, which reduce the self-interaction error by mixing in a fraction of Hartree-Fock exchange,[16,17] appear to resolve this problem of excessive delocalization of the O p_y lone-pair electrons in O-ZGNRs. With regard to accuracy of the hybrid functionals themselves, we note that Barone *et al.*[26,27] have shown in their studies on single-walled carbon nanotubes that the HSE06 functional yields more accurate band gaps than the PBE0 functional.[28] Given the similarity in many respects between carbon nanotubes and graphene, it is reasonable to expect that the band gaps obtained with the HSE06 functional in the present study are also more accurate than those obtained with the PBE0 functional; additional calculations with the GW method[29] ought to provide independent corroboration of the accuracy of the HSE06 functional.

Second, we see from Table I that O-ZGNRs are *thermodynamically stable* for all the cases considered here and have

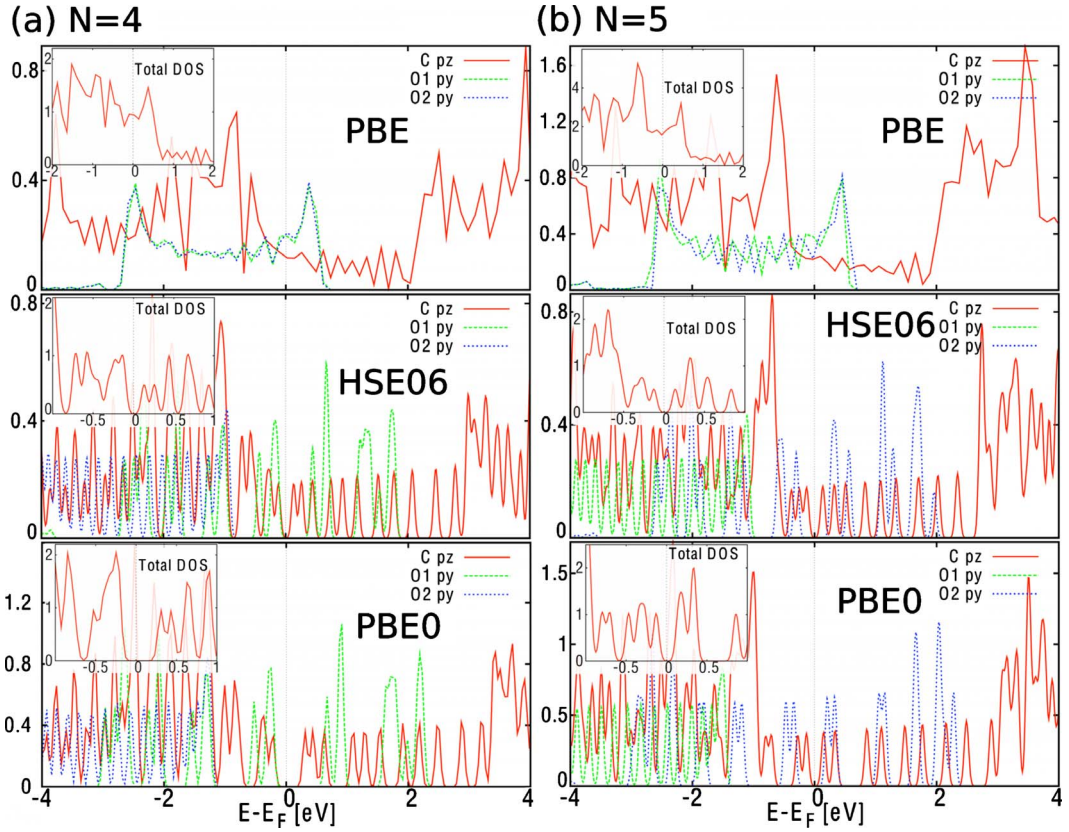

FIG. 3. (Color online) Partial and total (shown in insets) density of states for the (a) 4-O-ZGNR and (b) 5-O-ZGNR. Partial density of states are displayed for the p_y orbitals (lone pair) of the two edge O atoms and for the p_z orbitals summed over all C atoms. Since the two spin channels are degenerate, only the majority-spin channel is shown here.

also been reported to be stable for $N=8$ in previous work.[8] In contrast, the extensively studied H-ZGNRs (Refs. 6 and 9) are *weakly unstable* with respect to their constituents.[8] Thus, while H-ZGNRs might provide a useful model for studying the essential physics of ZGNRs they are not viable candidates for realistic applications. O-ZGNRs partially resolve this problem by being thermodynamically stable but by no means provide a panacea. An entirely different problem arises for O-ZGNRs wherein an appreciable band gap results only at extremely small sizes ($N=2-3$). Might it be possible to synthesize such narrow ZGNRs? While unzipping carbon nanotubes with an oxygen plasma[13,14] clearly cannot produce such narrow GNRs, recent experiments[30] have demonstrated the possibility of "thinning" GNRs via electron irradiation all the way down to single-atom carbon chains. Speculatively, combining this process of electron irradiation with controlled exposure to an oxygen plasma might facilitate synthesis of extremely narrow O-GNRs as could other techniques based on bottom-up chemical synthesis.

Finally, the disconcerting effects of self-interaction in standard DFT calculations with LSDA/GGA XC functionals, as clearly evidenced in this work, call for additional caution in electronic-structure studies of functionalized GNRs and graphene, especially when electrons are strongly localized on functional groups. Examples of such studies with LSDA/GGA abound (e.g., ketones, ethers, hydroxyl groups in Ref. 12; carboxyl, NO, NO_2 groups in Ref. 7; N, O, F adsorption on graphene in Ref. 31, among several others) and might require revisiting in light of this work.

IV. CONCLUDING REMARKS

In summary, I have investigated the size-dependent electronic properties of ultrathin O-ZGNRs ($N=2-5$ rows) using both standard and hybrid DFT calculations. The PBE XC functional within standard DFT and the PBE0 and HSE06 XC functionals within hybrid DFT were employed and contrasted in this study. The main conclusion is that, contrary to previous LSDA/GGA studies that predict metallic behavior for O-ZGNRs, hybrid DFT XC functionals predict semiconducting behavior for O-ZGNRs. This behavior is size dependent—the band gap decreases with increasing ribbon width and the ribbons essentially become zero band-gap semiconductors at $N=5$ with both PBE0 and HSE06 XC functionals. All ribbons with $N\geq 3$ rows display an antiferromagnetic ground state whereas the $N=2$ ribbon displays a nonmagnetic ground state. Through careful investigation of the electronic structure of the O-GNRs, we have seen that standard DFT calculations with the PBE XC functional display anomalous behavior by delocalizing the p_y lone pair of electrons from the O edge atoms. The delocalized lone pairs interact with the C p_z electrons and lead to a finite density of states at the Fermi level. These spurious states at the Fermi level are absent in the hybrid DFT calculations leading to the

presence of a clearly identifiable band gap. The unphysical behavior of the PBE XC functional may be attributed to the inherent self-interaction error of (semi)local XC functionals in standard DFT, which destabilizes localized Kohn-Sham orbitals such as those corresponding to electron lone pairs on atoms. In light of these findings, it would appear that caution must be exercised when studying the effect of lone-pair containing functional groups/atoms on GNRs and graphene, and in interpreting the results of previous investigations of such systems. Finally, we have seen that O-ZGNRs are thermodynamically stable and can exhibit appreciable band gaps, albeit at very small ribbon widths ($N=2-3$), which could be quite interesting from the perspective of molecular electronics.

ACKNOWLEDGMENTS

This research was supported in part by the National Science Foundation through TeraGrid resources provided by the Texas Advanced Computing Center under Grant No. TG-DMR090096. Useful conversations with Doron Naveh and Emily A. Carter are gratefully acknowledged.

*ashwin@engin.umass.edu

[1] A. K. Geim and K. Novoselov, Nature Mater. **6**, 183 (2007).
[2] A. H. Castro Neto, F. Guinea, N. M. R. Peres, K. S. Novoselov, and A. K. Geim, Rev. Mod. Phys. **81**, 109 (2009).
[3] Z. Chen, Y.-M. Lin, M. J. Rooks, and P. Avouris, Physica E (Amsterdam) **40**, 228 (2007).
[4] M. Y. Han, B. Özyilmaz, Y. Zhang, and P. Kim, Phys. Rev. Lett. **98**, 206805 (2007).
[5] D. Gunlycke, J. Li, J. W. Mintmire, and C. T. White, Appl. Phys. Lett. **91**, 112108 (2007).
[6] Y.-W. Son, M. L. Cohen, and S. G. Louie, Phys. Rev. Lett. **97**, 216803 (2006); Nature (London) **444**, 347 (2006).
[7] F. Cervantes-Sodi, G. Csányi, S. Piscanec, and A. C. Ferrari, Phys. Rev. B **77**, 165427 (2008).
[8] O. Hod, V. Barone, J. E. Peralta, and G. E. Scuseria, Nano Lett. **7**, 2295 (2007).
[9] D. Jiang, X.-Q. Chen, W. Luo, and W. A. Shelton, Chem. Phys. Lett. **483**, 120 (2009).
[10] X. Li, X. Wang, L. Zhang, S. Lee, and H. Dai, Science **319**, 1229 (2008).
[11] M. Fujita, K. Wakabayashi, K. Nakada, and K. Kusakabe, J. Phys. Soc. Jpn. **65**, 1920 (1996); K. Nakada, M. Fujita, G. Dresselhaus, and M. S. Dresselhaus, Phys. Rev. B **54**, 17954 (1996).
[12] G. Lee and K. Cho, Phys. Rev. B **79**, 165440 (2009).
[13] L. Jiao, L. Zhang, X. Wang, G. Diankov, and H. Dai, Nature (London) **458**, 877 (2009).
[14] A. Sinitskii, A. A. Fursina, D. V. Kosynkin, A. L. Higginbotham, D. Natelson, and J. M. Tour, Appl. Phys. Lett. **95**, 253108 (2009).
[15] The terminology "standard DFT," as used here, refers to the usual Kohn-Sham approach wherein the exchange-correlation potential is strictly (semi)local. In contrast, hybrid DFT contains a nonlocal Hartree-Fock-type exchange potential.
[16] S. Kümmel and L. Kronik, Rev. Mod. Phys. **80**, 3 (2008).
[17] B. G. Janesko, T. M. Henderson, and G. E. Scuseria, Phys. Chem. Chem. Phys. **11**, 443 (2009).
[18] G. Kresse and J. Furthmüller, Comput. Mater. Sci. **6**, 15 (1996); Phys. Rev. B **54**, 11169 (1996).
[19] P. E. Blöchl, Phys. Rev. B **50**, 17953 (1994).
[20] G. Kresse and D. Joubert, Phys. Rev. B **59**, 1758 (1999).
[21] J. P. Perdew, K. Burke, and M. Ernzerhof, Phys. Rev. Lett. **77**, 3865 (1996).
[22] J. P. Perdew, M. Ernzerhof, and K. Burke, J. Chem. Phys. **105**, 9982 (1996); M. Ernzerhof and G. E. Scuseria, *ibid.* **110**, 5029 (1999).
[23] J. Heyd, G. E. Scuseria, and M. Ernzerhof, J. Chem. Phys. **118**, 8207 (2003); **124**, 219906 (2006).
[24] The fact that this study finds a closing of the band gap at $N=5$, whereas Hod *et al.* still found a very small gap at $N=8$, is not a significant issue given that their work was carried out with a Gaussian basis set while this work was carried out with a plane-wave basis. The rather small gaps found with HSE06 for $N \geq 4$ are anyway within the level of expected error of the computational method. The main point that the O-ZGNR is semiconducting—possibly with a near zero band gap—rather than metallic still holds.
[25] N. Dori, M. Menon, L. Kilian, M. Sokolowski, L. Kronik, and E. Umbach, Phys. Rev. B **73**, 195208 (2006).
[26] V. Barone, J. E. Peralta, and G. E. Scuseria, Nano Lett. **5**, 1830 (2005).
[27] V. Barone, O. Hod, and G. E. Scuseria, Nano Lett. **6**, 2748 (2006).
[28] Rather than reproducing the fundamental gap, HSE06 actually seems to systematically approximate the quasiparticle excitation energy and reproduce the optical band gap (Ref. 32).
[29] M. S. Hybertsen and S. G. Louie, Phys. Rev. B **34**, 5390 (1986).
[30] C. Jin, H. Lan, L. Peng, K. Suenaga, and S. Iijima, Phys. Rev. Lett. **102**, 205501 (2009).
[31] M. Wu, E.-Z. Liu, and J. Z. Jiang, Appl. Phys. Lett. **93**, 082504 (2008).
[32] E. N. Brothers, A. F. Izmaylov, J. O. Normand, V. Barone, and G. E. Scuseria, J. Chem. Phys. **129**, 011102 (2008).